Extremely low inhomogeneous broadening of exciton lines in shallow (In,Ga)As/GaAs quantum wells

S.V. Poltavtsev [a,*], Yu.P. Efimov [b], Yu.K. Dolgikh [b], S.A. Eliseev [b],
V.V. Petrov [b], V.V. Ovsyankin [b]

[a] *Spin Optics Laboratory, St.-Petersburg State University, 1 Ul'anovskaya, Peterhof, St.-Petersburg 198504, Russia*
[b] *Department of physics, St.-Petersburg State University, 1 Ul'anovskaya, Peterhof, St.-Petersburg 198504, Russia*

ABSTRACT

We study radiative linewidth of exciton resonance in shallow $In_xGa_{1-x}As/GaAs$ single quantum wells as a function of indium concentration in the range $x = 0.02...0.10$ and well thickness in the range $L_Z = 1...30$ nm using method of Brewster reflection spectroscopy. Record linewidths of heavy-hole exciton resonance of about $130...180$ μeV are measured in reflection spectra for single quantum wells with $L_Z = 2$ nm and $x = 0.02$ at temperature of 9 K. In these spectra, the non-radiative linewidth including inhomogeneous broadening can be comparable or even less than radiative linewidth. It is shown that radiative linewidth weakly depends on x and L_Z in these ranges. In multiple-quantum-well Bragg structure with ten periods, the oscillator strength per individual quantum well is similar to that of single quantum well, while the total radiative linewidth exceeds inhomogeneous broadening by 4 times.

© 2014 Elsevier Ltd. All rights reserved.

1. Introduction

Semiconductor quantum-well-based devices play an important role in optical information transfer and laser technologies. The nano-structures with III–V quantum wells (QW) are considered as promising candidates to basic medium of future elements of information processing in a pure optical way [1,2]. In spite of the fact that molecular beam epitaxy (MBE) is highly developed, however, the quality of heterostructure growth achieved nowadays is insufficient for some perspective applications.

In the context of optical information processing, the most important properties of the QW system are the rate of resonant interaction with light and efficiency of coherence transfer from resonant light to quasi-2D excitons and back, from excitons to light. While the interaction rate is promisingly high due to the large oscillator strength of excitonic transitions in QWs, the coherence transfer is typically inefficient because of the dominant role of non-radiative damping processes. The coherence transfer efficiency can be expressed by the ratio of the radiative decay rate of excitons Γ_0 to the total decay rate of exciton ensemble including radiative and all non-radiative mechanisms (Γ_{NR}), such as exciton–phonon interaction, scattering on potential disorder and impurities, and spread of individual oscillator frequencies. For the

potential optical processing applications this ratio should be close to unity meaning dominant role of Γ_0.

To achieve this goal, two basic approaches seem feasible. The first one is reduction of role of exciton non-radiative damping mechanisms. While temperature-dependent exciton–phonon scattering can be sufficiently suppressed by cooling down the sample, the major non-radiative mechanism associated with the static potential disorder defined by the growth procedure remains. The reduction of inhomogeneity is a challenging task of MBE technology, and in this paper we demonstrate, in particular, that further technological efforts are reasonable.

The second approach is directed to the enhancement of oscillator strength linearly related to Γ_0. Two decades ago, Ivchenko and co-authors [3] suggested a conception of multiple-quantum-well Bragg structures with the QW layers separated by the half-wavelength period. It was theoretically shown that for the normal geometry of excitation, the oscillator strengths of individual QWs in these structures are accumulated and radiative part of reflection spectrum grows proportionally to the number of QWs, N. Later on, it was experimentally demonstrated that in $In_{0.04}Ga_{0.96}As$ MQW Bragg structures the total linewidth in reflection spectrum, indeed, grows linearly up to $N = 100$, and the reflection coefficient reaches 95%, for samples with anti-reflection coating and normal geometry of measurement [4]. Sample with $N = 210$ demonstrates close to 100% reflection [5]. Time-resolved measurements by the four-wave-mixing revealed the presence of fast decaying super-radiant component from high-quality $N = 10$ MQW Bragg structure confirming

* Corresponding author.
E-mail address: svp@bk.ru (S.V. Poltavtsev).

efficient radiative coupling of excitons in different QWs [6]. While the radiative linewidth increases linearly with N, the non-radiative broadening is associated with fluctuating nature of local inhomogeneity and increases sub-linearly. The influence of disorder on absorption spectrum of MQW Bragg structure is carefully studied in theory [7].

In this paper, we report on results obtained with reflection spectroscopy performed at $T = 9$ K on a set of (In,Ga)As/GaAs single quantum well (SQW) structures demonstrating extremely low inhomogeneous broadening of excitonic lines comparable with radiative linewidth. Background-free reflection spectra measured in Brewster geometry exhibit exciton linewidths as narrow as 130…180 μeV. We also study $N = 10$ MQW Bragg structure, for which simulation of reflection spectrum gives the radiative linewidth of individual QWs similar to that measured for SQWs, while the total radiative linewidth exceeds by four times the broadening of exciton line.

2. Experimental method and theoretical model

To measure reflectivity spectra from the QW samples the Brewster angle geometry and femtosecond laser pulses have been exploited. The samples were mounted in a closed-cycle cryostat and cooled down to 9 K. The linearly polarized laser beam was focused on a spot of about 50×150 μm at the Brewster angle, $\alpha_{Br} = 74.5° \pm 0.5°$. The reflected beam was focused on the open slit (≈ 0.5 mm) of a 0.6-m spectrometer with grating 1200 lines/mm, equipped with CCD at the output. Spectral resolution provided by the set-up is 20 μeV. The wide spectrum of 100-fs pulses of the Ti:sapphire laser (Tsunami) allowed one to cover all spectral features of interest in the sample. Intensity of fs-pulses used in the experiment was checked to lie in the range of linear excitation regime.

The samples under study were 20 (In,Ga)As/GaAs heterostructures comprising total 36 SQWs and one $N = 10$ MQW Bragg structure grown on (100) GaAs substrates. The growth conditions and sample structure were optimized during the manufacturing and characterization processes, which resulted in the following simple scheme used for all high-quality samples: GaAs substrate was overgrown by ~ 1 μm-thick GaAs buffer layer followed by one to five $In_xGa_{1-x}As$ QW layers with $L_Z = 1/31$ nm separated by 50/110 nm-thick GaAs barriers and terminated by GaAs cap layer. Indium concentration in the QW layers was ranging between 0.02 and 0.10. The sample of MQW structure (P555) was composed of ten 3 nm-thick $In_{0.02}Ga_{0.98}As$ QWs separated by 110 nm-thick barriers nominally satisfying Bragg conditions. The samples were grown without substrate rotation and possess a high spatial inhomogeneity of spectral properties caused by a variation of layer thicknesses and indium concentration.

To simulate experimental reflection spectra we used the transfer matrix method based on several approximations. First, we neglect the difference of background permittivity ε_0 of different layers, since we see no reflection far from any resonances. Second, we exploit Lorentz approximation implying that all mechanisms of exciton ensemble relaxation can be characterized by certain relaxation rates, including spread of individual oscillator frequencies, which leads to inhomogeneous broadening. In case of significant inhomogeneity, this approximation would be insufficient and analysis based on non-local dielectric response, given for instance in [8,9], would be required. Here in our study, we consider this inhomogeneity to be insufficient to distort Lorentz line shape of absorption. To describe resonant features we used the following local effective single-pole dielectric function [10,11]:

$$\varepsilon(\omega) = \varepsilon_0 + \varepsilon_0 \omega_{eff}/(\omega_0 - \omega - i\Gamma_{NR}), \quad \omega_{eff} = 2\Gamma_0/\sin(\omega\sqrt{\varepsilon_0}L_Z/c). \tag{1}$$

Here, ω_0 is the heavy-hole exciton resonance frequency, ω is the light frequency, Γ_0 and Γ_{NR} are the radiative and non-radiative decay rates of excitons, respectively, ω_{eff} is the effective longitudinal-transverse splitting of excitons, and c is the speed of light. In particular cases, when the exciton line is an isolated peak in background-free spectrum, its shape is typically very well fitted with Lorentz line allowing one to conduct a simple analysis as it has been done previously on GaAs SQW [12]. The resonance shape can be described then with the simple formula taking into account the finite angle of light incidence φ ($\approx 16°$) onto the QW layer inside the structure [3,13]:

$$R(\omega) = \frac{\Gamma_0^2 \cos^2\varphi}{(\omega - \omega_0)^2 + (\Gamma_0 \cos\varphi + \Gamma_{NR})^2}. \tag{2}$$

Using resonant reflection coefficient $K_{RR} = R(\omega_0)$ and the value of full-width at half-maximum (FWHM) of the exciton line Γ, we can obtain radiative and non-radiative exciton linewidths, which we associate with exciton decay rates accordingly:

$$K_{RR} = \Gamma_0^2 \cos^2\varphi/\Gamma^2, \tag{3}$$

$$\Gamma = \Gamma_0 \cos\varphi + \Gamma_{NR}, \quad K_{RR} = 1/(1 + \Gamma_{NR}/\Gamma_0 \cos\varphi)^2, \tag{4}$$

$$\Gamma_0 = \Gamma\sqrt{K_{RR}}/\cos\varphi, \quad \Gamma_{NR} = \Gamma(1 - \sqrt{K_{RR}}). \tag{5}$$
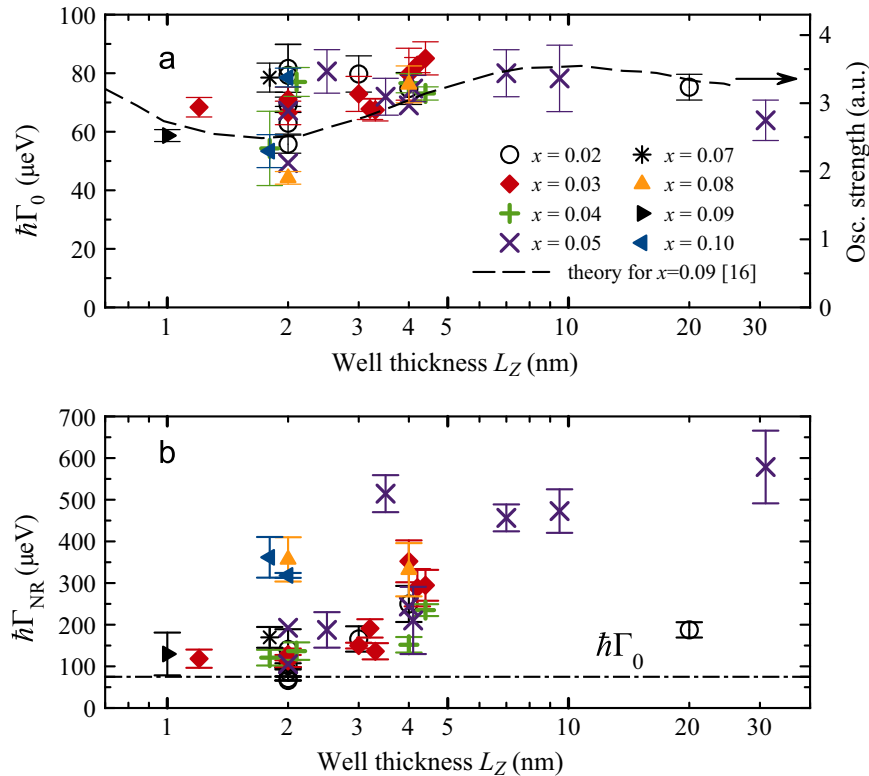
3. Experimental results and discussion

3.1. Resonant reflection from SQW

A set of reflection spectra was measured in different spots of each sample. The samples with SQW nominally having $L_Z < 4$ nm and indium concentration $x < 0.04$ demonstrate the most narrow exciton lines. Spectra from the four most perfect SQW samples P550, P554, P566, and P561 are presented in Fig. 2(a)–(d) by red solid lines. Typical spectrum displays heavy-hole (HH), light-hole (LH) as well as higher energy exciton transitions located around the GaAs bulk exciton resonance ($E > 1.514$ eV). The presented spectra demonstrate exciton linewidths narrower than those reported in the literature [12,14,5,15]. In particular, the heavy-hole exciton line for the sample P554 has FWHM $\hbar\Gamma = 130$ μeV [Fig. 1(b)] and for the sample P561 $\hbar\Gamma = 152$ μeV [Fig. 1(d)]. We note that these linewidths include temperature-dependent part, which can be extracted by measuring the temperature dependence of reflection [12]. It was experimentally checked that this broadening is $\hbar\Gamma_2 \approx 13$ μeV for $T = 9$ K and linearly depends on temperature up to 40 K with a coefficient of about 1.5 μeV/K.

For all reflection spectra resonant features related to the lowest heavy-hole exciton transition from each SQW were analyzed. For the case of isolated resonant lines, Lorentz approximation was applied to extract values of resonant reflection coefficient K_{RR} and resonance linewidth Γ; then, Eqs. (5) were used to calculate radiative and non-radiative linewidths. The spectra containing a number of resonant lines were simulated with the transform matrix method to obtain the same quantities, Γ_0 and Γ_{NR}. The simulated spectra are shown in Fig. 1(a)–(d) with black dashed lines. The results of experimental measurements of Γ_0 and Γ_{NR} as a function of QW thickness and indium concentration are presented in Fig. 2. They reveal weak dependence of Γ_0 on both parameters smoothed by the measurement scatter, and can be approximated by a constant value $\hbar\Gamma_0 \approx 75$ μeV. Our experimental results are in good qualitative agreement with the theoretical calculations of exciton oscillator strength performed for (In,Ga)As/GaAs SQW [16]. Although error of each experimental point averaged over 6/8 spectra is rather small due to high local homogeneity of studied quantum wells, there is some scatter of
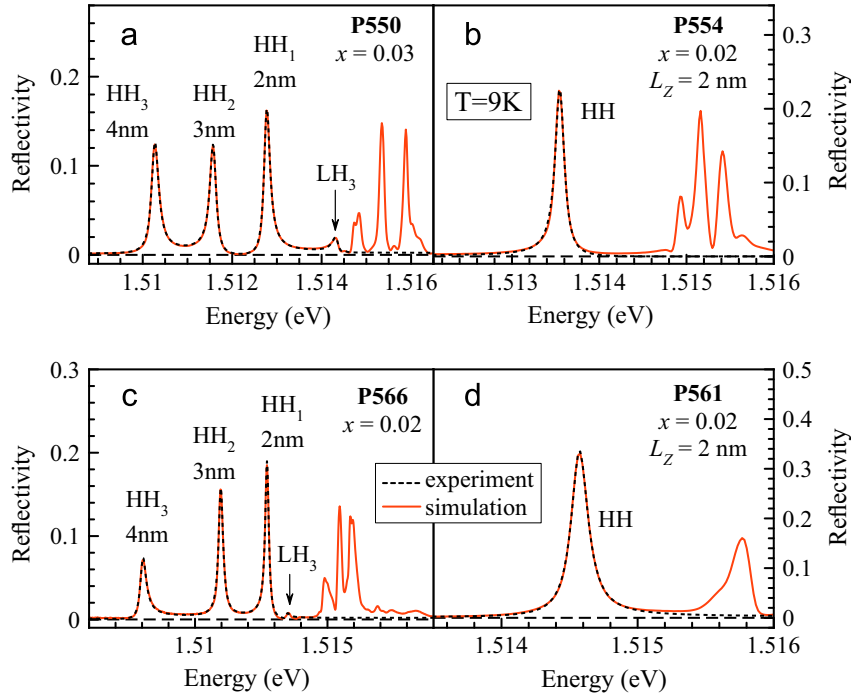
Fig. 1. (Color online) Reflectivity spectra of the four SQW samples with a number of SQW with indicated thicknesses (*red solid* – experiment; *black dash* – simulation.): (a) sample P550: $\hbar\Gamma$ (QW1) = 170 µeV, $\hbar\Gamma$ (QW2) = 181 µeV, $\hbar\Gamma$ (QW3) = 211 µeV; (b) sample P554: $\hbar\Gamma$ = 130 µeV; (c) sample P566: $\hbar\Gamma$ (QW1) = 178 µeV, $\hbar\Gamma$ (QW2) = 217 µeV, $\hbar\Gamma$ (QW3) = 307 µeV; (d) sample P561: $\hbar\Gamma$ = 152 µeV.


Fig. 2. (Color online) Experimental dependence of (a) exciton radiative linewidth and (b) non-radiative linewidth on QW thickness and indium concentration obtained on SQW samples. *Dashed* line in (a) is the theoretically calculated oscillator strength taken from [16]. *Dash-dotted* line in (b) is averaged value of measured $\hbar\Gamma_0$ (75 µeV).

points, which we ascribe to a random deviation between nominal and real QW layer thicknesses and indium concentrations.

The fact that Γ_0 is practically universal property of reflection spectra measured on different (In,Ga)As/GaAs QWs results in simplification of Eq. (4) connecting now the amplitude of exciton

resonant line, K_{RR}, with the broadening factor Γ_{NR}. Thus, one may compare both quantities among different QWs. According to our measurements, the lowest Γ_{NR} is achieved on quantum wells having 2 nm thickness and indium concentration of about 0.02. On a number of samples, we obtained Γ_{NR} comparable to Γ_0 or
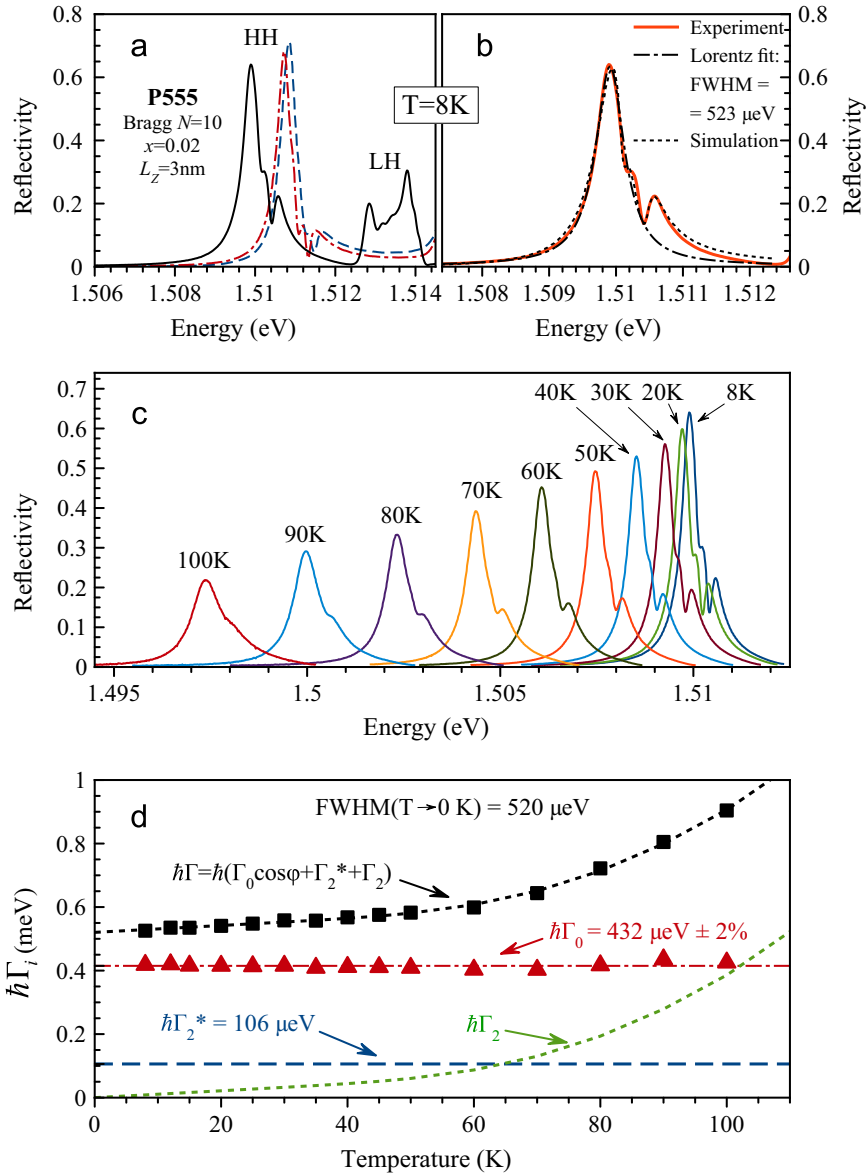
Fig. 3. (Color online) Reflection spectroscopy of the MQW Bragg structure: (a) the reflection spectra taken at $T=8$ K at different spots; (b) simulation of experimental spectrum (*red solid*) by fitting with simple Lorentzian (*blue dash-dot*) and using the transfer matrix method (*black dot*); (c) the reflection spectrum as a function of temperature; (d) experimental temperature dependence of Lorentz FWHM (*black squares*), fitting with Eqs. (6) (*black dash*), radiative linewidth, $\hbar\Gamma_0$ (*red triangles with dash-dotted guide*), inhomogeneous broadening, $\hbar\Gamma_2^*$ (*blue dash*), and homogeneous broadening, $\hbar\Gamma_2$ (*green dash*).

even less, as it is seen from Fig. 2(b). According to Eq. (4), when $\Gamma_{NR} = \Gamma_0 \cos\varphi$ theoretical value of the reflection coefficient K_{RR} is 0.25. In the P561 sample, the reflection amplitude reaches value 0.32 and $\Gamma_{NR} = 0.76\Gamma_0$. The main result we obtained here is approaching of inhomogeneous broadening to a minimal value with decreasing of (In,Ga)As/GaAs QW thickness, which is opposite to the case of (Al,Ga)As/GaAs QWs, for which diminishing of QW thickness causes the larger penetration of the exciton wave-function to the disordered ternary alloy of the barriers giving rise to the higher inhomogeneity. In case of (In,Ga)As structures, narrowing of QW layer leads to the escape of exciton wave-function from the disordered InGaAs region to the GaAs barrier with subsequent decrease of inhomogeneity.

3.2. Reflection from MQW Bragg structure

To get enhanced reflection from quantum well, we used the MQW Bragg structure. The sample P555 containing $N=10$ spatially periodic

3 nm QWs with indium concentration $x=0.02$ has been designed to perform high efficient reflection in the Brewster geometry. Since no substrate rotation during the growth process was used, the sample had spatial gradient in optical properties and, hence, possessed a pronounced inhomogeneity. It was possible, however, to locate a macroscopic area of the sample, where Bragg condition, i.e. separation of QW layers by half-wavelength period, was fulfilled. The spectra presented in Fig. 3(a) were measured at different sample spots and demonstrate resonant reflection coefficient up to 0.7. The spectrum presented with black solid line was analyzed with transfer matrix method described above using minimal number of free parameters. The simulation result is shown in Fig. 3(b) with the black dotted line together with original spectrum (red solid). Deviation of the real spectrum from the Lorentz shape can be explained by two assumptions, which we employ: (1) there is a small mismatch of MQW spatial period responsible for the slight shape distortion; (2) one of ten QWs is split-off the main resonance, thus, leading to an additional peak at the right tail of resonant line. For all SQWs the

value of radiative linewidth was set equal. Also, nine top QWs were supposed to have equal non-radiative linewidths, energy positions and barrier thicknesses. These parameters for the tenth (deepest) QW were left free. Consequent fitting procedure gave value $\hbar\Gamma_0 = 71$ µeV for radiative linewidth of each QW, which is in good agreement with the results obtained on a set of SQW structures. Deviation within 2% is achieved between the fitted spatial MQW period (115 nm) and the Bragg period calculated for the Brewster geometry: $\lambda/2n_0 \cos\varphi = 112.8$ nm, where $\lambda = 821$ nm is resonant wavelength, $n_0 \approx 3.5$ is GaAs refractive index.

The spectrum under consideration can be satisfactorily approximated by a simple Lorentzian [dash-dotted line in Fig. 3(b)] with FWHM = 523 µeV characterizing the super-radiant mode linewidth. Within this simplified approximation, we may perform further analysis of the resonant line structure based on measurements of reflection spectrum as a function of temperature [12]. This method allows one to extract the radiative linewidth of the super-radiant mode and to separate non-radiative linewidth onto temperature-dependent homogeneous broadening $\Gamma_2(T)$ and inhomogeneous broadening Γ_2^*. Evolution of the reflection spectrum measured at the same spot with increasing temperature is displayed in Fig. 3(c). With rising temperature, exciton line decreases in amplitude, becomes broader and experiences red shift. Measured FWHM of the exciton line as a function of temperature is displayed in Fig. 3(d) with black squares. It can be fitted with the following expression considering that only Γ_2 is temperature-dependent [17]:

$$\Gamma(T) = \Gamma_0 \cos\varphi + \Gamma_2^* + \Gamma_2(T),$$
$$\Gamma_2(T) = \gamma_{ac}T + \Gamma_{LO}/\left[\exp(\hbar\omega_{LO}/k_B T) - 1\right], \tag{6}$$

where $\hbar\gamma_{ac} = 1.1$ µeV/K and $\hbar\Gamma_{LO} = 11.5$ meV are fitted coupling constants of exciton-acoustic-phonon and the exciton-optical-phonon interactions, $\hbar\omega_{LO} \approx 36$ meV is the optical phonon frequency in GaAs [18], and k_B is the Boltzmann constant.

Using Eqs. (5) and (6), the radiative as well as non-radiative linewidths can be extracted: $\hbar\Gamma_0 = 432$ µeV, $\hbar\Gamma_2^* = 106$ µeV. These values are shown in Fig. 3(d) by red triangles and blue dashed line, respectively. The fact that Γ_0 appeared to be a well-fixed constant serves as a reliable argument that we are dealing with a single oscillator (super-radiant mode) possessing enhanced oscillator strength. The radiative decay rate of this super-radiant mode is about four times higher than the rate of non-radiative damping caused by the inhomogeneity.

To extract the individual QW contribution Γ_0' to the total radiative linewidth of the super-radiant mode, we may use the following function describing the line shape [19]:

$$R(\omega) = \frac{(N\Gamma_0' \cos\varphi)^2}{(\omega - \omega_0)^2 + (N\Gamma_0' \cos\varphi + \Gamma_{NR})^2} \tag{7}$$

here, $N = 9$ is the number of QWs involved in the enhanced reflection. From here we get $\hbar\Gamma_0' \approx 48$ µeV, which is somewhat smaller than the value, calculated with the transfer matrix method (71 µeV). This difference, as we assume, comes from the mismatch of the real spacing between QWs with calculated Bragg-period resulting in loss of super-radiant mode efficiency.

We can compare our results with the data obtained by Prineas et al. [4,15] on a set of 8.5 nm In$_{0.04}$Ga$_{0.96}$As/GaAs MQW Bragg structures having anti-reflection coating and studied in the normal incidence geometry. The authors have demonstrated linear growth of total linewidth for increasing QW number N. For $N = 10$ the resonant reflection coefficient was about 0.36 and FWHM ≈ 1 meV, which are quite different as compared to the values obtained on our sample (0.7 and 0.52 meV, respectively). We believe, this difference comes from the relatively strong inhomogeneous broadening present in the spectra shown in [4,15]. We assume that this inhomogeneity is conditioned by the larger thickness of QWs (8.5 nm) and higher

indium concentration (0.04) as compared to 3 nm and 0.02, respectively, in our case.

4. Conclusion

In conclusion, we have performed reflection spectroscopy from shallow InGaAs QWs and MQW Bragg structure in the Brewster angle geometry. Background-free spectra of QWs with low concentration of indium demonstrate heavy-hole exciton resonances with linewidth below 0.2 meV and resonant reflection coefficient up to 0.32 proving equal roles of the radiative and non-radiative mechanisms of exciton decay. We have shown that the dependence of oscillator strength on SQW thickness and indium concentration within 0.02–0.10 is weak. On high-quality MQW Bragg structure we have studied the enhancement of radiative contribution to the resonance linewidth. We have checked that the resultant super-radiant mode behaves as a single oscillator conserving its oscillator strength at temperature ranging between 8 and 100 K. Both considered possibilities of increasing the role of the radiative contribution to the exciton linewidth are important for application of QW-based materials in optical processing and storage devices, for which efficiency of the coherence transfer in the process of mutual exciton–photon interconversion as well as high non-linearity are the key properties [1,2]. QWs featuring narrow exciton lines are also appealing for fast switching applications and devices requiring a dense spectral lines design.

References

[1] I.Y. Gerlovin, V.V. Ovsyankin, B.V. Stroganov, V.S. Zapasskii, Nanotechnology 11 (2000) 383.
[2] I.Y. Gerlovin, V.V. Ovsyankin, B.V. Stroganov, V.S. Zapasskii, J. Lumin. 87–89 (2000) 421.
[3] E. Ivchenko, A. Nesvizhskii, S. Jorda, Superlattices Microstruct. 16 (1994) 17.
[4] J.P. Prineas, C. Ell, E.S. Lee, G. Khitrova, H.M. Gibbs, S.W. Koch, Phys. Rev. B 61 (2000) 13863.
[5] J.P. Prineas, C. Cao, M. Yildirim, W. Johnston, M. Reddy, J. Appl. Phys. 100 (2006) 063101.
[6] M. Hübner, J. Kuhl, T. Stroucken, A. Knorr, S. Koch, R. Hey, K. Ploog, Phys. Rev. Lett. 76 (1996) 4199.
[7] V. Kosobukin, A. Poddubnyǐ, Phys. Solid State 49 (2007) 1977.
[8] G. Malpuech, A. Kavokin, J. Leymarie, P. Disseix, A. Vasson, Phys. Rev. B 60 (1999) 13298.
[9] L.C. Andreani, G. Panzarini, A.V. Kavokin, M.R. Vladimirova, Phys. Rev. B 57 (1998) 4670.
[10] E. Ivchenko, V. Kochereshko, P. Kop'ev, V. Kosobukin, I. Uraltsev, D. Yakovlev, Solid State Commun. 70 (1989) 529.
[11] E. Ivchenko, Harrow, Alpha Science International Ltd., UK, 2005.
[12] S.V. Poltavtsev, B.V. Stroganov, Phys. Solid State 52 (2010) 1899.
[13] L.C. Andreani, F. Tassone, F. Bassani, Solid State Commun. 77 (1991) 641.
[14] B. Zhang, S. Kano, Y. Shiraki, R. Ito, Phys. Rev. B 50 (1994) 7499.
[15] M. Hübner, J.P. Prineas, C. Ell, P. Brick, E.S. Lee, G. Khitrova, H.M. Gibbs, S.W. Koch, Phys. Rev. Lett. 83 (1999) 2841.
[16] A. D'Andrea, N. Tomassini, L. Ferrari, M. Righini, S. Selci, M. Bruni, D. Schiumarini, M. Simeone, J. Appl. Phys. 83 (1998) 7920.
[17] J. Lee, E.S. Koteles, M.O. Vassell, Phys. Rev. B 33 (1986) 5512.
[18] H.R. Chandrasekhar, A.K. Ramdas, Phys. Rev. B 21 (1980) 1511.
[19] E. Ivchenko, V. Kochereshko, A. Platonov, D. Yakovlev, A. Waag, W. Ossau, G. Landwehr, Phys. Solid State 39 (1997) 1852.